Development and application of the 3D-SPH surface erosion model to simulate multiple and overlapping impacts by angular particles

* X.W. Dong[1], Zengliang Li[1]

[1]College of mechanical and electronic engineering, China University of Petroleum, 66 Changjiang Rd, Huangdao District, Qingdao, China

*Presenting author: dongxw139@163.com
†Corresponding author: dongxw139@163.com

Abstract

This paper presents a 3D smoothed particle hydrodynamics (SPH) modeling procedure to simulate surface erosion of ductile materials subjected to impacts of angular particles. Our SPH model is a meshfree, Lagrangian particle method, based on the standard SPH formulation, and the materials are discretized with a set of particles, in which the targeted ductile material is modeled as an elastic-plastic material, and the angular particles are modeled as a rigid bodys. The present SPH has been improved developing SPH formulations for the Johnson-Cook's plasticity model and failure model to describe plastic behavior and ductile fracture process. The particle interactions between the angular particles and targeted material are taken into account by employing a contact algorithm. Our SPH erosion model is applied to simulate multiple and overlapping impacts of particles on ductile targets. Two modified schemes in terms of density correction and kernel gradient correction are adopted to improve the accuracy of the SPH approximation. Besides, stabilities are ensured using artificial viscosity and density correction, and the numerical oscillations in conventional SPH method are effectively suppressed. The present SPH method and algorithm are then further performed to model solid particle erosion process. The results are compared with available experimental data, and good agreement has been achieved. It is demonstrated that the present SPH procedure is superior to the conventional numerical methods in treating problems of extremely large deformations and with breakages, which usually occurs in the surface erosion process by angular particles.

Keywords: 3D smoothed particle hydrodynamics (SPH); surface erosion; angular particles; multiple and overlapping impacts; kernel gradient correction

1.Introduction

The material removal caused by impacts of particles is generally described as surface erosion by impacts. Impact onductile materials using foreign particlesmay be viewed as either constructive useful engineering technique (e.g. shot blasting[1], abrasive jet[2]) or destructive harmful processes (e.g. impeller erosion[3], pipe erosion[4, 5]. Study of the mechanisms of surface erosion by impacts is helpful in promoting this engineering technique effectively or reducing possible erosive wear.

Material deformation and removal are two main material behaviors involved in surface erosion by impacts. For ductile material, the impacts of the foreign particles cause localized plastic strain[6, **15**] at the contact site on the surface and material is removed when the strain exceed a threshold value[7]. It has been known that material removal does not necessarily occur during the process of foreign particles impacting on ductile targets. It depends on many factors[9**,**5**,19,22**], some of which may individually or synthetically determine the erosion mechanisms, such as particle velocity, angle of attack, particle shape and size of particle, etc. Besides, these erosive factors also affect removal rate of targeted material, i.e., erosion rate. Usually, correlations between erosion rate and erosive factors are obtained through experiments by measuring mass loss or analyzing eroded surface. However, the interaction of these factors makes it difficult to take a close look at the mechanisms experimentally. For example, it is hard to observe the dynamic process of material removal (also called material spallation) or analyze the dependency on some single erosive factor through experiment due to the process is too fast and complex. Computer modeling allows studying the effect of factors separately. And, as a complement to experiment, it can obtain detail informations by controlling the simulation procedure, which can help to reveal the fundamental behaviors involved in the erosion process and predict the erosion performace with respect to different erosive factors.

Early computation models tried to build the correlations between erosion rate and concerned erosive variables[8−**14**,**19**,**21**]. These models simplified the eroded ductile targets as elastic–perfectly plastic materials, of which the yield stress is assumed to be constant. However, the targeted materials would endure high–strain–rate deformation during the short time of real process of surface erosion, especially by hard and angular particle[**15−17**]. The yield stress is rate–dependent rather than a constant[**18**, **20**]. Therefore, these models can only obtain correct results after tuning parameters by experiments, which then limited their developments and applications.

Finite element method (FEM) is an effective numerical method in solving completed problems in solid mechanics and has been applied widely to model the surface erosion impacted by spherical particles[7, **23**−**28**]. With appropriate constitutive material models, FEM is capable to simulate the relevant damage phenomena in surface erosion process. These models can be validated by experimental observations or analytical solutions. However, these FEM models mainly focused on predictions of erosion rate quantitatively or analysis of erosion mechanisms qualitatively. It is difficult to observe and reveal the erosion mechanisms for these FE models due to the poorly simulating of dynamic process of material removal. Moreover, actual foreign particles usually have complex geometry shape with angularity. Impacts of angular particle can cause large plastic deformation and rapid material removal, which may result in the heavily distorted elements with poor quality. Thereofore, standard FEM may be not suitable for modelling surface erosion by impacts involving large plastic deformation and material removal. Takaffoli[**12**] proposed a new model for modeling impact of angular particle on OFHC Copper. The model is able to handle these damage behaviors using techniques of adaptive re–meshing and element erosion. Although these techniques overcome the element distortion problems in FE model, they are computationally expensive and may lead to numerical instabilities, especially for multiple overlapping impacts. It can be concluded that these difficulties originate from grid limitation. Almost all the grid–based numerical methods have the difficulties to handle large deformation and material removal.

Smoothed particle hydrodynamics (SPH) is a Lagrangian meshfree particle method. It was initially developed for astrophysical problems[**29**−**31**]. Since its invention, SPH has been extensively applied in the many fields of science and engineering including fluid mechanics and solid mechanics, such as free surface flows [**32**,**33**], viscous flow[**34**,**35**], high velocity impacts[**36**−**38**], geophysical flows[**39**,**40**], etc. As a meshfree method, SPH does not need a mesh or elements to discretize computation domain. Instead of nodes, particles are adopted to carry the field variables such as mass, density, stress, and to approximate the governing equations. These particles have a spatial distance (named as the “smoothing length”), over which their properties are “smoothed” by a kernel function. SPH has great advantages over the grid–based numerical methods to deal with large deformation and material removal due to its adaptive nature[**40**]. Then, SPH method may be a better option to simulation of surface erosion by impacts.

In the past few years, several preliminary applications of SPH method to surface erosion by impacts have been performed andsome encouraging results have been obtained. For example, Wang and Yang [**41**] investigated multiple impacts spherical particles on Ti–6AL–4V under the scheme of SPH method. The predicted erosion dependency on impact factors agrees well with the analytical and experimental results. However, this study focused on predictions of erosion ratewithoutdemonstrating the advantageous of SPH over conventional numerical method. Takaffoli[**42**] proposed a SPH model to simulate the impact of single angular particles on AL6061–T6 targets. This model implemented Johnson–Cook flow stress and failure model. The dynamic process of material removal caused by impacts was first revealed and the resluts showed that SPH method can account for both material deformation and chip separation. It demonstrated that the SPH method is able to capture the major fundamental dynamic behavior of surface erosion by impacts. However, the traditional SPH method encounters the problem of low accuracy as the accuracy is closely related to the distribution of particles[**43**, **44**]. Also, another crucial aspect is the phenomena of numerical oscillations, which highly affect the numerical stability of the SPH calculation[**38**, **45**].

This paper is to establish a general SPH framework for modeling surface erosion by impacts which comprises reproduction of material behavior in terms of both plastic deformation and material removal and improvement of numerical stability/accuracy. It is then necessary to extend of the SPH method to handle general material constitutive models with plastic flow rules and material failure. In Section 2, the general concepts of the SPH modelling for continuum material are given, and the SPH formulations are presented. Two modified schemes for density correction and kernel gradient correction are then implemented. This paper provides a general approach to resolve the material constitutive relations in SPH, in which small time step ensures the constitutive relations be computed correctly. In Section 3, the model is applied to simulate impacts of diamond particles on *OFHC Copper* and AL6061-T6 surface. Firstly, the SPH model is validated by reproducing the experimental data from published literature. Secondly, the validated model is used to simulate the multiple and overlapping impacts. The impact behaviors related to overlapping impacts are investigated by particularly selecting the impact points of the particles. Thirdly, the multiple and overlapping impacts are simulated by using randomly distributed impact points.

2. SPH surface erosion model

2.1 Model description

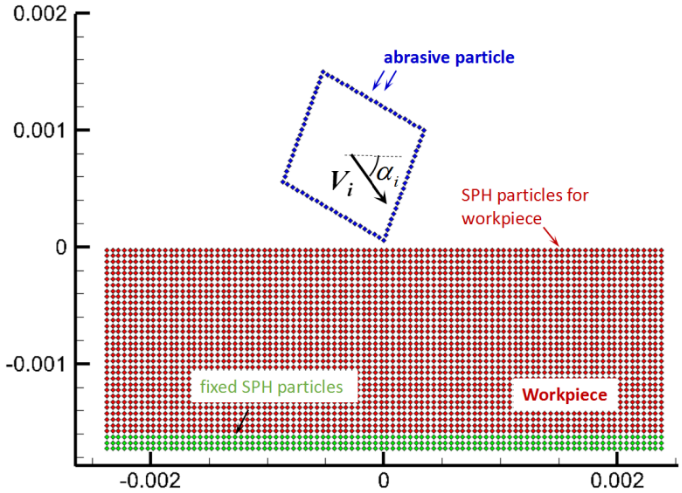

Fig1.Single angular particle impact on targeted material

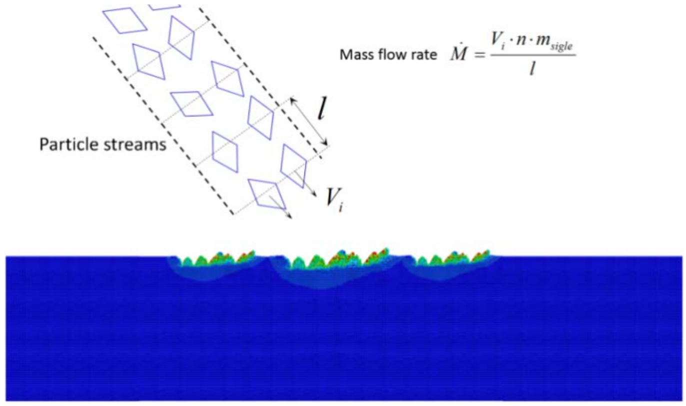

Fig2.Many angular particle impact on targeted material resulting in multiple and overlapping impacts

In this paper, surface erosion by impacts is modeled based on the rigid–plastic theory[57, 59]. Targeted materials which may have large deformation and chip separation are represented and discretized by SPH particles (not the 'angular particle'), and the angular particle is treated as rigid body assuming it is hard enough to keep non–deformable during erosion process.

Fig1 shows the initial geometry of the two dimensional model of surface erosion by impact, in which angular particle is given a velocity and the targeted material is in steady state with the velocity and stress being zero at the initial time. The bottom particles are held fixed during the simulation to realize displacement boundary condition. Besides, in order to eliminate the effect of model width (L), periodic boundary conditions were prescribed on the side faces of the target block. As shown in Fig.1, the use of periodic boundary conditions assume an infinite plate in width direction. Moreover, the dimensions of the targeted block

(L,W) should also be determined so that the impact simulations would be not affected by edge effects.

The rigid foreign particle, as shown in Fig1, is discretized by one layer of ‘surface particles’. The interaction between foreign particle and targeted material is considered by applying a particle contact algorithm developing for meshfree method. The proposed rigid–plastic SPH model allows the simulation of the entire event of particle impact with respect to different erosive factors (eg. impact velocity, angle of attack, particle shape etc.), including dynamic process of interaction between angular particle and targeted material, the particle kinematics in terms of rebound behavior and particle trajectory, the erosion performance.

2.2 Governing equations and SPH formulations

The governing equations of ductile targeted material which consist of mass and momentum conservation equations can be expressed following

$$\frac{D\rho}{Dt} = -\rho \frac{\partial v^{\alpha}}{\partial x^{\alpha}} \tag{1}$$

$$\frac{Dv^{\alpha}}{Dt} = \frac{1}{\rho}\frac{\partial \sigma^{\alpha\beta}}{\partial x^{\beta}} + f^{\alpha} \tag{2}$$

where α and β denote the Cartesian components x, y with the Einstein convention applied to repeated indices; ρ is the material density; t is the time; v is the velocity; $\sigma^{\alpha\beta}$ stands for the total stress tensor; the total stress tensor $\sigma^{\alpha\beta}$ has two parts, one is isotropic pressure p and the other one is deviatoric shear stress $\tau^{\alpha\beta}$; f^{α} is the component of acceleration caused by external force.

To solve the above governing equations in the SPH framework, one has to approximate these equations using SPH interpolation functions. Since the computation domain has been discretized by particles, the field function at a particle can be obtained simply through summations over all particles within the support domain of the particle using a kernel weighting function, of which the process is so–called particle approximation. The particle approximation for a function and its spatial derivatives at a particle $i$can be expressed in the form as

$$\langle f(\boldsymbol{x}_i)\rangle = \sum_{j=1}^{N} \frac{m_j}{\rho_j} f(\boldsymbol{x}_j) \cdot W(x_i - x_j, h) \tag{3}$$

$$\langle \nabla \cdot f(\boldsymbol{x}_i) \rangle = -\sum_{j=1}^{N} \frac{m_j}{\rho_j} f(\boldsymbol{x}_j) \cdot \nabla_i W_{ij} \tag{4}$$

where $W(x_i - x_j, h)$ the smoothing function or kernel function, and $\nabla_i W_{ij}$is gradient of kernel, $\nabla_i W_{ij} = \frac{\mathrm{x_i - x_j}}{\mathrm{r_{ij}}} \frac{\partial \mathrm{W_{ij}}}{\partial \mathrm{r_{ij}}} = \frac{\mathrm{x_{ij}}}{\mathrm{r_{ij}}} \frac{\partial \mathrm{W_{ij}}}{\partial \mathrm{r_{ij}}}$

According to the continuity equation (Eq.(1) and momentum equation (Eq.2), the governing equations can be expressed as[**46**]

$$\begin{cases} \dfrac{d\rho_i}{dt} = \rho_i \sum_{j=1}^{n} \dfrac{m_j}{\rho_j} v_{ji}^{\beta} \cdot \dfrac{\partial W_{ij}}{\partial x_i^{\beta}} \\ \dfrac{dv_i^{\alpha}}{dt} = \sum_{j=1}^{n} m_j \dfrac{\sigma_i^{\alpha\beta} + \sigma_j^{\alpha\beta}}{\rho_i \rho_j} \cdot \dfrac{\partial W_{ij}}{\partial x_i^{\beta}} + f_i^{\alpha} \\ \dfrac{de}{dt} = \dfrac{1}{2} \sum_{j=1}^{n} m_j \left(\dfrac{P_i + P_j}{\rho_i \rho_j} \right) v_{ij}^{\beta} \cdot \dfrac{\partial W_{ij}}{\partial x_i^{\beta}} + \dfrac{\tau_i^{\alpha\beta} \varepsilon_i^{\alpha\beta}}{\rho_i} \\ \dfrac{dx_i^{\alpha}}{dt} = v_i^{\alpha} \end{cases} \tag{5}$$

where *e* is internal energy, *p* is isotropic pressure, $\tau^{\alpha\beta}$ is deviatoric shear stress, $\varepsilon^{\alpha\beta}$is strain rate tensor.

In SPH, there are many possible choices of the smoothing function W in Eq(**3)**–(**5)**. The cubic spline function, which was originally proposed by Monaghan and Lattanzio[**47**], has been the most widely used smoothing function in the published SPH literatures since it closely resembles a Gaussian function while having a narrower compact support[**37**]. The cubic spline function is used in this study

$$W_{ij} = \alpha_d \times \begin{cases} \dfrac{2}{3} - q^2 + \dfrac{1}{2} q^3, & 0 \le q < 1 \\ \dfrac{1}{6} (2 - q)^3, & 1 \le q < 2 \end{cases} \tag{6}$$

where α_d is the normalization factor, which is $15/(7\pi \mathrm{h}^2)$ for 2D problem and q is the normalized distance between particle *i* and *j* defined as $q = r_{ij}/h$. r_{ij} is the distance between particle *i* and *j*.

As discussed above, the total stress tensor $\sigma^{\alpha\beta}$ was decomposed into two parts: an volumetric part *p* (named ‘pressure’ in this paper) and a deviatoric shear stress $\tau^{\alpha\beta}$

$$\sigma^{\alpha\beta} = -p\delta^{\alpha\beta} + \tau^{\alpha\beta} \tag{7}$$

In this paper, the pressure (P) is computed by means of an equation of state (EOS). The Mie–Gruneisen equation, which has been shown to be suitable for solid materials under compressive shock loading[**38**], is employed to describe pressure–volume–energy behavior of ductile materials under particle impact. The pressure is related to density and internal energy in the form of $P = P(\rho, e)$.

For elastic solid of dynamics, the shear stress (τ) can be integrated by time following the incremental formulation of Hooke's law, in which the linear elastic relation between stress and deformation tensors has been derived in time. In order to guarantee the independence from rigid rotations, the Jaumann rate is adopted here with the following elastic constitutive equation as[**46**]

$$\frac{d\tau^{\alpha\beta}}{dt} = 2G\left(\dot{\varepsilon}^{\alpha\beta} - \frac{1}{3}\delta^{\alpha\beta}\dot{\varepsilon}^{\gamma\gamma}\right) + \tau^{\alpha\gamma} \cdot \dot{r}^{\beta\gamma} + \tau^{\gamma\beta} \cdot \dot{r}^{\alpha\gamma} \tag{8}$$

where G is the shear modulus of the concerned material, $\dot{\varepsilon}^{\alpha\beta}$ is the strain rate tensor given by

$$\dot{\varepsilon}^{\alpha\beta} = \frac{1}{2}\left(\frac{\partial v^{\alpha}}{\partial x^{\beta}} + \frac{\partial v^{\beta}}{\partial x^{\alpha}}\right) \tag{9}$$

$\dot{r}^{\alpha\beta}$is the rotation rate tensor defined through

$$\dot{r}^{\alpha\beta} = \frac{1}{2}\left(\frac{\partial v^{\alpha}}{\partial x^{\beta}} - \frac{\partial v^{\beta}}{\partial x^{\alpha}}\right) \tag{10}$$

The above elastic constitutive relations can be extended to plastic behavior based on the von Mises yield criterion

$$f_y = \frac{\sigma_y}{\sigma_{vM}} < 1 \tag{11}$$

where σ_{vM} is von Mises equivalent stress, σ_y is yield stress. When the von Mises yield criterion is met ($f_y < 1$) the material is considered to be yielded and a plastic behavior is identified. Then the stress tensor is scaled back to the yield surface. For the elastic–perfectly plastic material, the yield stress is considered to be constant. However, the eroded targets can not be treated as elastic–perfectly plastic material due to the yield stress is rate–dependent. In this paper, the Johnson–Cook flow stress model[**55**], which is one of the most popular consititutive models for numerical simulations of impact, is adopted to account for rate–dependent plastic behavior of eroded ductile targets. Johnson–Cook flow stress model is a purely empirical model and can accout for strain rate hardening and thermal softening. The yield stress in Johnson–Cook model can be written as

$$\sigma_y = \left[A + B\left(\varepsilon_{eff}^{p}\right)^{N}\right]\left[1 + Cln\left(\frac{\dot{\varepsilon}_{eff}^{p}}{\dot{\varepsilon}_0}\right)\right]\left[1 - (T^*)^M\right] \tag{12}$$

where ε_{eff}^{p} is the equivalent plastic strain, $\dot{\varepsilon}_{eff}^{p}$ is the equivalent plastic strain rate, $\dot{\varepsilon}_0$ is reference equivalent plastic strain rate, and *A*, *B*, *C*, *N*, and M are material dependent constants. The normalized temperature (T^*) is given by

$$T^* = \frac{T - T_{ref}}{T_{melt} - T_{ref}} \tag{13}$$

where T_{ref} is reference temperature, T_{melt} is melting temperature of concerned material, and real temperature *T*is calculated by a simplified thermal mechanical coupling equation

$$T = \frac{\varphi W_p}{\rho C_p} + T_{ref} \tag{14}$$

where W_p is the plastic work, φ is the coefficient represents the fraction of the plastic work changing to heat, C_p is the specific heat of concerned material.

In order to model the material removal due to impact of angular particles, it is necessary to employ a failure model. Here, a cumulative–damage failure model, which was also proposed by Johnson and Cook [**56**], is adopted to simulate material removal during the impact process. In the failure model, a parameter *D* is introduced to measure the local damage state and given by

$$D = \sum \frac{\Delta\varepsilon_{eff}^{P}}{\varepsilon_{failure}} \tag{15}$$

where $\Delta\varepsilon_{eff}^{p}$ is the increment of equivalent plastic strain occurring during an integration cycle and $\varepsilon_{\mathrm{failure}}$ is the equivalent strain to failure given by

$$\varepsilon_{failure} = \left[D_1 + D_2 exp(D_3\sigma^*)\right]\left[1 + D_4 ln\left(\frac{\dot{\varepsilon}_{eff}^{p}}{\dot{\varepsilon}_0}\right)\right]\left[1 + D_5 T^*\right] \tag{16}$$

where $D_1 - D_5$ are material constants, $\sigma^*$is defined as the ratio of the mean stress σ_m to the von Mises equivalent stress σ_{vM}.

When parameter D is greater than 1, the material failure is considered to occur and the corresponding stress is reduced to zero, which considers the reduction of stress level due to the material failure.

To solve above constitutive relations, i.e. Eq. (**7**)~(**16**), two steps are proposed. Firstly, the equations should be discretized into the SPH framework for every particle. For example, the strain and rotation rate tensors (Eq.(**9**), Eq.(**10**)) of a particle are discretized into the SPH formulations given by

$$\varepsilon_i^{\alpha\beta} = \frac{1}{2}\sum_{j=1}^{N}\left(\frac{m_j}{\rho_j} v_{ji}^{\alpha}\frac{\partial W_{ij}}{\partial x_i^{\beta}} + \frac{m_j}{\rho_j} v_{ji}^{\beta}\frac{\partial W_{ij}}{\partial x_i^{\alpha}}\right) \tag{17}$$

$$r_i^{\alpha\beta} = \frac{1}{2}\sum_{j=1}^{N}\left(\frac{m_j}{\rho_j} v_{ji}^{\alpha}\frac{\partial W_{ij}}{\partial x_i^{\beta}} - \frac{m_j}{\rho_j} v_{ji}^{\beta}\frac{\partial W_{ij}}{\partial x_i^{\alpha}}\right) \tag{18}$$

Then, the discretized equations and corresponding variables are interpolated and updated following the updated Lagrangian formulations. Besides, the procedure of stress–rescaling and judgment of failure are performed during every integration cycle following the corresponding criterion we presented above. This paper adopt a very small timestep in the explicitly updated Largrangian procedure, which can reduce the inaccuracy of incrementally updating the stress state following the constitutive relations.

2.3 Corrective terms

In this paper, two modified schemes in terms of density correction and kernel gradient correction are adopted, which have been proved effectively to improve computational accuracy[**33**, **53**, **54**]. For the density correction, we adopt a so–called Moving Least Squares(MLS)[**49**] approach, which is a interpolation scheme on irregularly scattered points. This scheme has been applied successfully by Colagrossi and Landrini[**53**] in SPH dam break simulation. And the linear variation of the density field can be exactly reproduced by using this first order correction scheme to correct the density. Besides, it is found that for the cases with irregular particle distribution a smoother pressure field can be obtained through MLS density correction, which may be helpful in improving the stability in this simulation. Herein, we use MLS approach to correct the density field as

$$\langle\rho_i\rangle = \sum_{j}\rho_j W_{ij}^{MLS} V_j = \sum\nolimits_{j} m_j W_{ij}^{MLS} \tag{19}$$

where the moving–least–square kernel W_j^{MLS} is computed through (for 3D problem)

$$\begin{cases} W_{ij}^{MLS} = [\beta_0(\boldsymbol{x}_i) + \beta_1(\boldsymbol{x}_i)x_{ij} + \beta_2(\boldsymbol{x}_i)y_{ij} + \beta_3(\boldsymbol{x}_i)z_{ij}]W_{ij} \\ \beta(\boldsymbol{x}_i) = [\beta_0\ \beta_1\ \beta_2 \beta_3]^T = A(\boldsymbol{x}_i)[1\ 0\ 0\ 0]^T \\ A(\boldsymbol{x}_i) = \left[\sum_j W_{ij} \begin{bmatrix} 1 & x_{ij} & y_{ij} & z_{ij} \\ x_{ij} & (x_{ij})^2 & x_{ij}.y_{ij} & x_{ij}.z_{ij} \\ y_{ij} & x_{ij}.y_{ij} & (y_{ij})^2 & y_{ij}z_{ij} \\ z_{ij} & x_{ij}.z_{ij} & y_{ij}z_{ij} & (z_{ij})^2 \end{bmatrix} V_j \right]^{-1} \end{cases} \tag{20}$$

where $V_j (= \mathrm{m_j}/\mathrm{\rho_j})$ is the volume of particle j. It should be noted that the density is still integrated by time using continuity equation(Eq. (**1**)) and density correction is applied periodically.

As to kernel gradient correction, the accuracy is restored with the following correction on the kernel gradient by multiplying the original kernel gradient with a matrix $L(r_i)$, which is obtained from Taylor series expansion method [**33**]. In two dimensional spaces, the new kernel gradient can be obtained as follows

$$\nabla_i^{new} W_{ij} = L(r_i)\nabla_i W_{ij} \tag{21}$$

where $x_{ji} = x_j - x_i$, $y_{ji} = y_j - y_i$. It has been proved that the SPH particle approximation scheme with kernel gradient correction is of second order accuracyfor general cases with irregular particle distribution[**33**, **54**].

Then, the standard SPH formulation of momentum equation is rewritten based on our improved method in the following way

$$\frac{dv_i^\alpha}{dt} = \sum_{j=1}^{N} m_j \left[-\left(\frac{P_i + P_j}{\rho_i \rho_j}\right)\delta^{\alpha\beta} + \frac{\sigma_i^{\alpha\beta} + \sigma_j^{\alpha\beta}}{\rho_i \rho_j} + \Pi_{ij}\delta^{\alpha\beta} \right] \frac{\partial W_{ij}^{new}}{\partial x_i^\beta} + f_i^\alpha \tag{22}$$

where the last term(Π_{ij}) between brackets is called artificial viscosity and is used to reduce the unphysical oscillations in the numerical results around the shocked region[**46**]. Of several proposals for artificial viscosity developed so far, the most widely applied is derived by Monaghan[**31**]

$$\Pi_{ij} = \begin{cases} \dfrac{-\alpha \bar{c}_{ij}\mu_{ij} + \beta\mu_{ij}^2}{\bar{\rho}_{ij}} & \vec{V}_{ij}\cdot\vec{x}_{ij} < 0 \\ 0 & \vec{V}_{ij}\cdot\vec{x}_{ij} \geq 0 \end{cases} \tag{23}$$

where $\mu_{ij} = \frac{h_{ij}(\vec{V}_{ij} \cdot \vec{x}_{ij})}{|\vec{x}_{ij}|^2 + 0.01h_{ij}^2}$, $\bar{c}_{ij} = (c_i + c_j)/2$, $\bar{\rho}_{ij} = (\rho_i + \rho_j)/2$, $h_{ij} = (h_i + h_j)/2$, c is the speed of sound, h is the smoothing length; $\alpha,\ \beta$ are constants and should be chosen according to particular applications.

It should be note that for our improved SPH formulations only kernel and kernel gradient are modified. And a field function and its derivatives are approximated separately as the standard SPH method does, which means that there is no need to change the procedure of computation of previous standard SPH. The main structure of SPH code remains unchanged. Therefore, it is relatively convenient to implement above improved SPH formulations.

2.4 Time integration scheme

The discrete SPH formulations are generated for every particle in the form of ordinary differential equations as described above. In order to solve these ordinary differential equations, time integration scheme is used to integrate the field variables. In this work, the Leap Frog (LF) algorithm is adopted due to its low memory requirement and high efficiency. In LF algorithm, the field variables are updated by using the following equations:

$$\rho_{n+1/2} = \rho_{n-1/2} + \left(\frac{d\rho}{dt}\right)_n \cdot \Delta t \tag{24}$$

$$v_{n+1/2}^{\alpha} = v_{n-1/2}^{\alpha} + \left(\frac{dv^{\alpha}}{dt}\right)_n \cdot \Delta t \tag{25}$$

$$\tau_{n+1/2}^{\alpha\beta} = \tau_{n-1/2}^{\alpha\beta} + \left(\frac{d\tau^{\alpha\beta}}{dt}\right)_n \cdot \Delta t \tag{26}$$

$$x_{n+1}^{\alpha} = x_n^{\alpha} + v_{n+1/2}^{\alpha} \cdot \Delta t \tag{27}$$

where Δt is time step length.

The stability of the above LF integration scheme is governed by the CFL(Courant–Friedrichs–Levy) contidition

$$\Delta t \leq 0.2\frac{h}{c} \tag{28}$$

where c is sound speed of the concerned material.

According to basic principles presented above, a SPH procedure and code are established based on the SPH code written in Fortran[46].

3.Simulation of multiple and overlapping impacts using well-defined particles

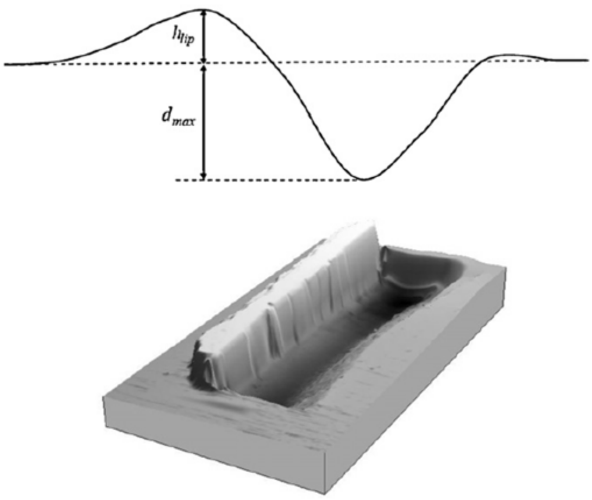

Fig. 1. Typical crater profile resulted by a well-defined angular particle[42]

3.1 Single impact and multiple impact

In this section, we simulate the impact of single angular particle on ductile surface (OFHC Copper and Al6061-T6). The Johnson-Cook parameters of two ductile materials are listed in Table.1. Smulation of single particle helps to validate the numerical model using available experimental results of single impact test. For example, M.Takaffoli and M.Papini[12] studied the single diamond particle impact on OFHC Copper. In their experiment, the launching device was specially designed to realize the adjustment of incident conditions of single particle such as initial orientation (θ_i), impact angle (α_i) and impact velocity (v_i). Figure 1 shows the definitions of incident parameters, geometry parameters and rebound parameters. In this section, we use the same test configuration as the experiment and the predicted results are compared with experimental data, then model validation could be performed.

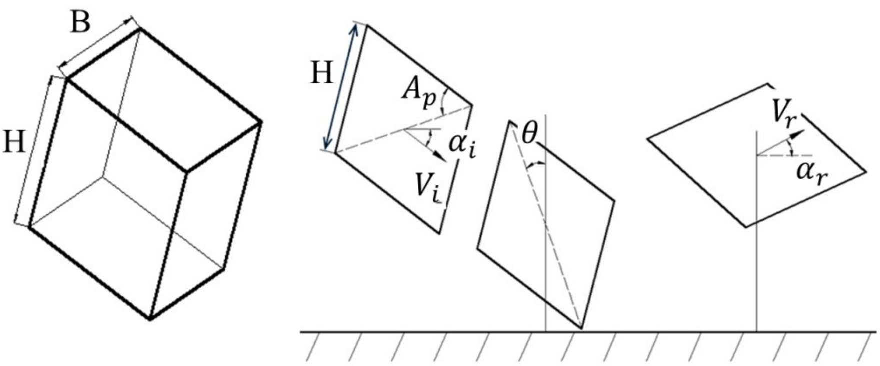

Fig. 2. Geometry, incident, rebound parameters of foreign particle

Table. 1 **Material parameters for Johnson-Cook model**

Material type	A (MPa)	B (MPa)	n	C	m
AL6061-T6	324	114	0.42	0.002	1.34
OFHC Copper	90	292	0.31	0.025	1.09

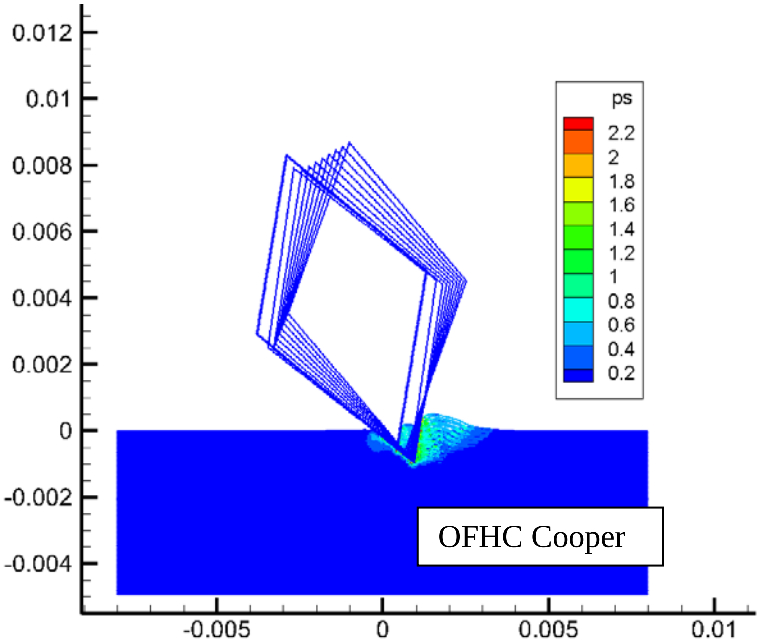

Fig. 3. Dynamic impact process of single angular particle (time interval 10µs)

$$v_i = 81m/s \ \alpha_i = 60^{\circ}, \theta_i = 20^{\circ}$$

Figure 2 shows the simulated impact process of diamond shaped particle on OFHC Copper. The length of the particle size is 5.46mm, the impact velocity is 81m/s. As shown in the figure, the particle impacts on the surface at an oblique impact angle (60°) resulting in an asymmetric erosive crater. In Fig. 3, the predicted crater is compared to measured crater profile, which shows that the predicted crater profile matches well with measured data. It illustrates the model could effectively and accurately obtained reliable results, which ensures further application on multiple and overlapping impact simulation.

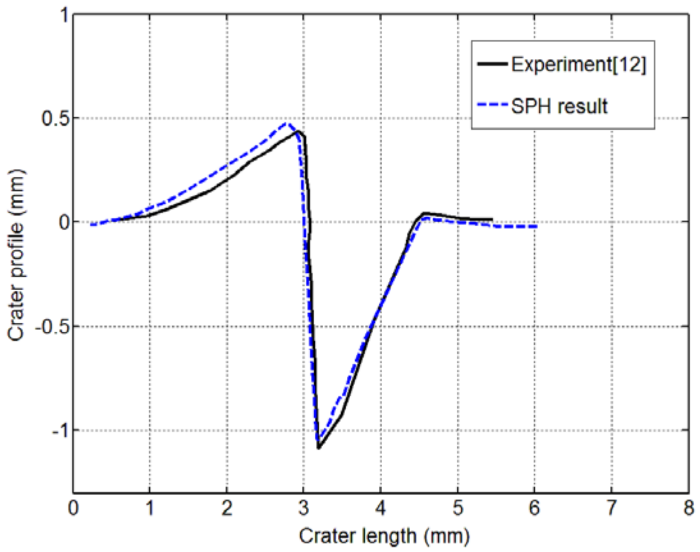

Fig. 4.Single particle impact on OFHC Copper surface at $v_i = 81m/s$ $\alpha_i = 60^\circ$, $\theta_i = 20^\circ$

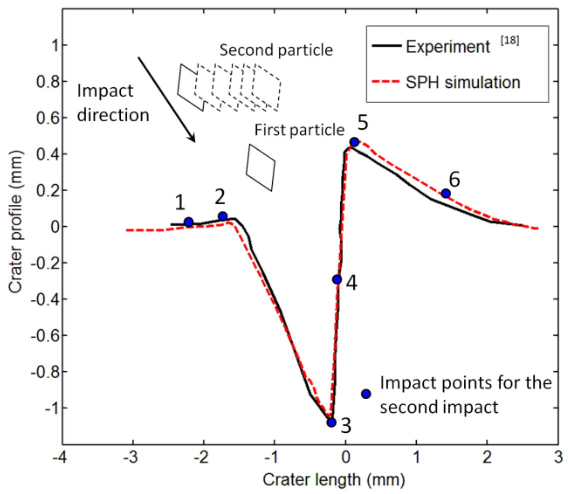

Fig. 5. Second particle impact on previous crater: illustration of different impact points for the second particles $(\theta_i = 20°, \alpha_i = 60°, V_i = 80\mathrm{m/s})$

In surface erosion process, impact on piled-up material is usually considered as the main mechanism of material removal when particles repeatedly impact on the surface. In order to simplify the problem and reveal the fundamental process, two impacts are considered in one simulation. In other words, two angular particles given same incident conditions impact on the surface successively to make sure overlapping impact occur. Then, we investigate the effect of previously resulted crater on the impact behavior and erosion mechanism of subsequent impact. Figure 4 presents the predicted crater profile caused by the first impact and the corresponding measured profile[12]. It shows good agreement both in crater shape and dimensions.

As shown in Fig.4, six impact points are particularly selected for the second particle along the crater surface resulted from the first impact. Accordingly, six predicted craters of overlapping impacts are obtained and shown in Fig.5. The crater profile of the first impact (black line) is also plotted in the figure for comparison purposes.

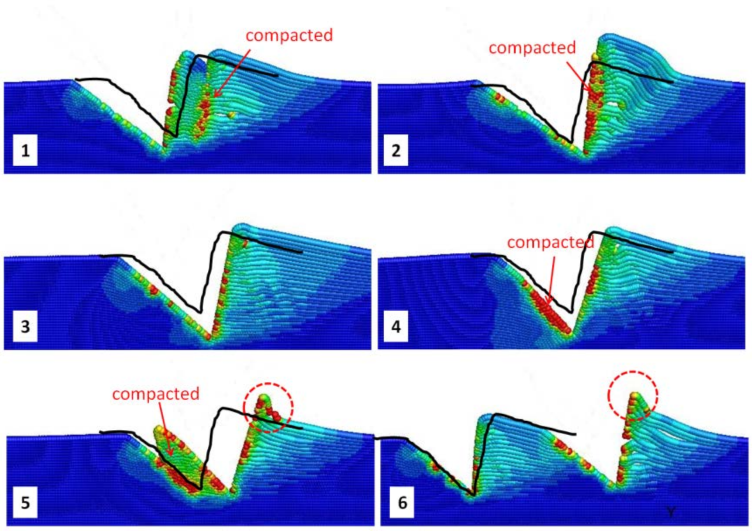

Fig. 6. Erosive craters by overlapping impacts of two particles (black line represents crater profile by the first impact)

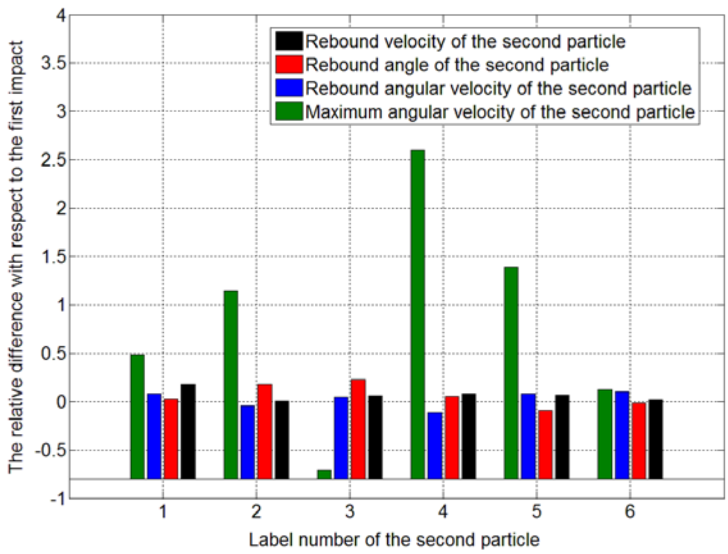

Fig. 7 Illustration of effect of location of impact point on the parameters related to particle motion

Figure 6 illustrates the effect of impact point on the predicted parameters of particle motion including v_r, α_r, ω_r and ω_{max}. It can be clearly seen that the influence of impact point on the maximum angular velocity (ω_{max}) is bigger than that on any other predicted variables. It means that the existing crater (the first crater) highly influences the initially generated particle rotation, including not only the magnitude but also the rotation direction. For example, for the impact of number 4, the second particle impacts on the inner side of the crater, as shown in Fig.5, the actual θ_i relative to the contact surface is a negative value which results in particle tumbling forward with a far higher ω_{max}(up to 250% higher) than the first impact. Compared with ω_{max}, other variables (v_r, α_r, ω_r) have smaller change when changing the impact point. It should be noted that these three variables are all rebound parameters, of which α_r is mostly heavily affected with the maximum difference up to 25% (Number 3).

3.2 Multiple and overlapping impacts using random impact points

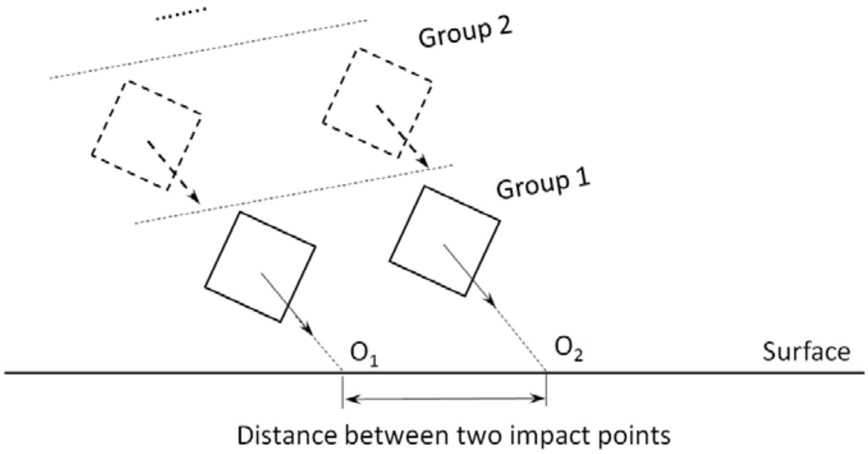

Fig. 8 Group of particles impact on the surface

Real particle erosion system usually involves many particles impact on component surface randomly. In order to reproduce the erosion process as realistic as possible, a random multiple impact model is proposed in this section. As shown in Fig.7, particles are launched to impact on surface group by group, each group contains several particles (two particle in this study). Total particles number is calculated by multiplying group number with particle number in one group. The random characteristic is realized through assigning a random impact point for each particle.

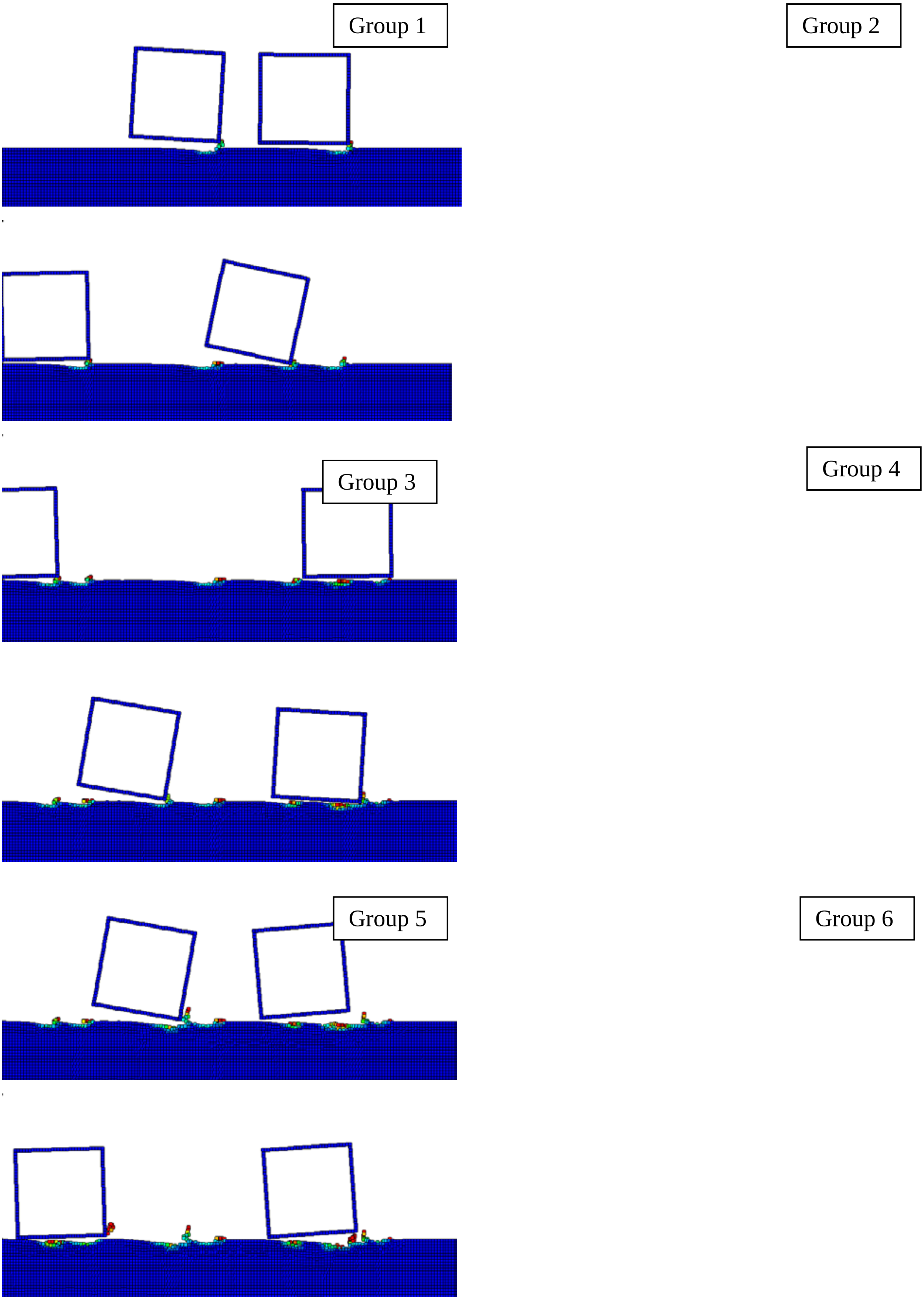

Fig. 9 Six group of particles impact on surface successively

In Fig.8, six group of particles impact on the surface successively. As discussed above, the impact point for each particle in one group is randomly selected. Therefore, overlapping impact may occur when successive particle just impacts on the craters caused by previous particles. Overlapping impacts make the surface materials continuously deform and damage is cumulated until failure occurs, which result in severe deformation on the surface. As shown in Fig.9, overlapping impacts increase the surface roughness. Besides, in the overlapping impact process, chip separation is likely to occur due to the gross failure of the chip materials.

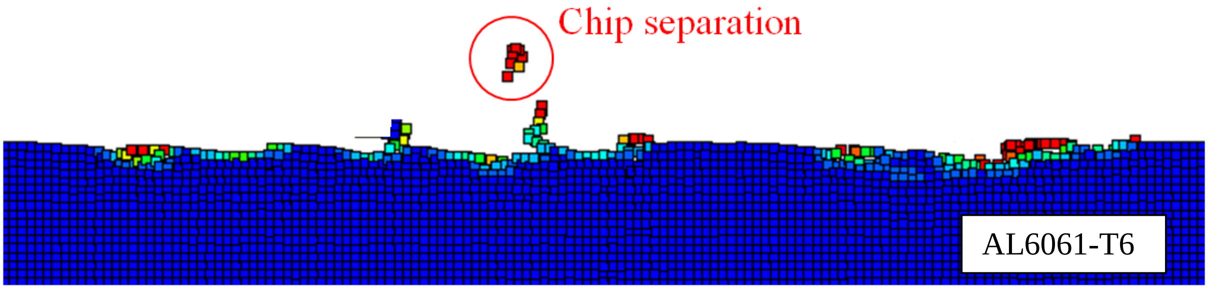

Fig. 10 Surface morphology resulted by 15 particles impact ($\theta_i = 39°$, $\alpha_i = 51°$, $V_i = 60\mathrm{m/s}$)

In Fig.9, same incident conditions ($\theta_i = 39°$, $\alpha_i = 51°$, $V_i = 60\mathrm{m/s}$) are assigned for all 15 particles. Even though incident conditions do not keep constant in real erosion process (such as θ_i), it is reasonable to assume the particles have same incident conditions (especially for impact angle and impact velocity) in order for comparative study.

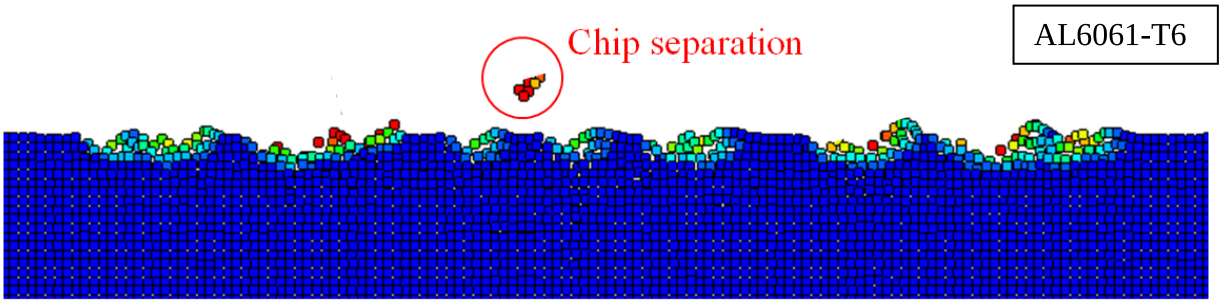

Fig. 11 Surface morphology resulted by 20 particles impact ($\theta_i = 0°$, $\alpha_i = 30°$, $V_i = 60\mathrm{m/s}$)

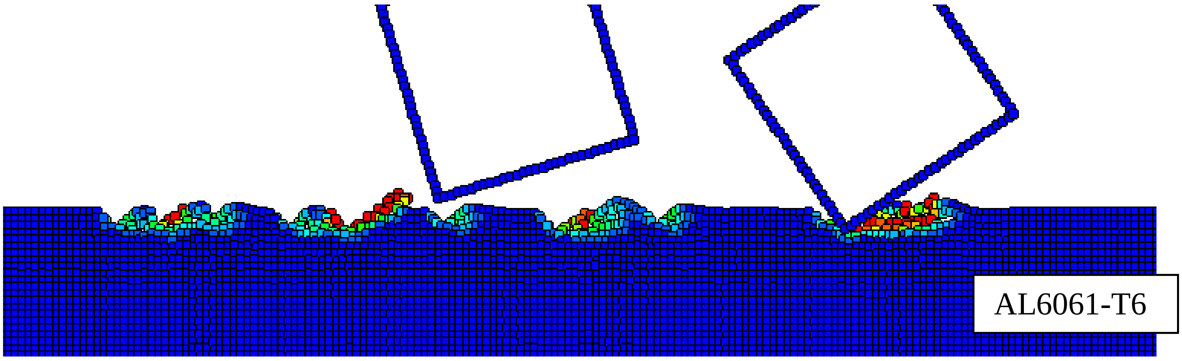

Fig. 12 Surface morphology resulted by 20 particles impact ($\theta_i = 0°$, $\alpha_i = 40°$, $V_i = 60\mathrm{m/s}$)

In Fig.10 and Fig.11, 20 particles impact on the surface at $\theta_\mathrm{i} = 0°$, at $\alpha_\mathrm{i} = 30°$ or $\alpha_\mathrm{i} = 40°$ and at $\mathrm{V_i} = 60\mathrm{m/s}$. Figure 12 (a) and (b) show 40 particles impact on the surface using the same incident conditions in Fig.11. Overlapping impacts make surface materials fail and the failed materials (SPH particles) are still maintained on the surface due to this study assume hydrostatic pressure could have negative value. The failed materials could be removed for better observation of the broken surface, as shown in Fig.12(b).

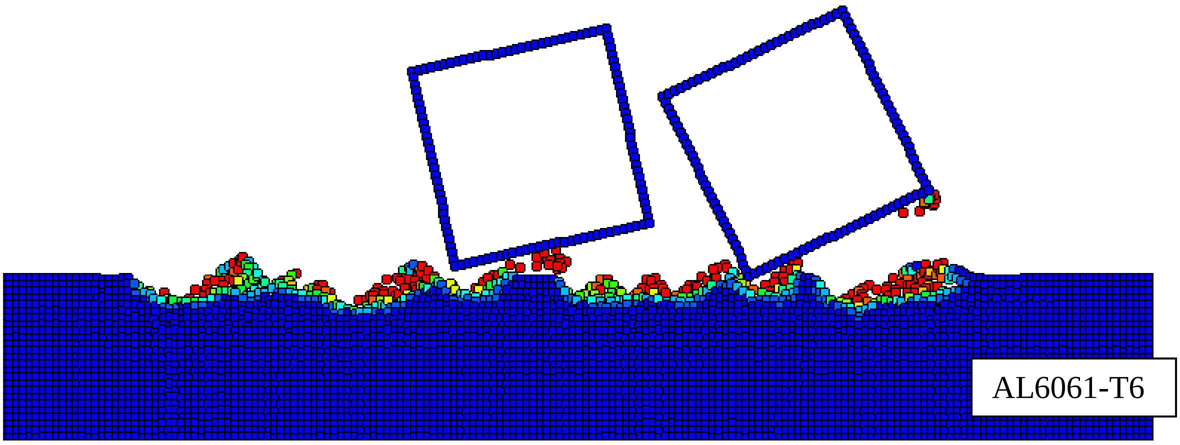

(a)

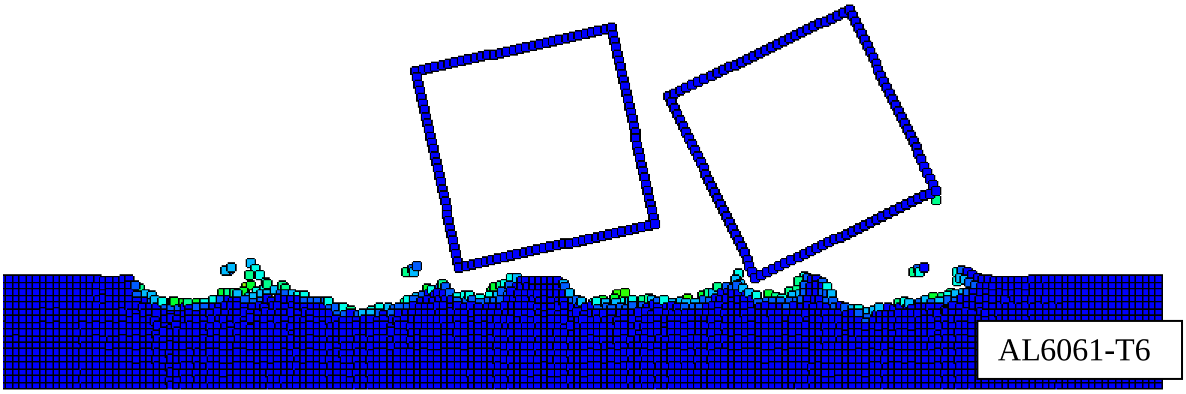

(b)

Fig. 13 Surface morphology resulted by 40 particles impact $(\theta_i = 0°, \alpha_i = 40°, V_i = 60\mathrm{m/s})$

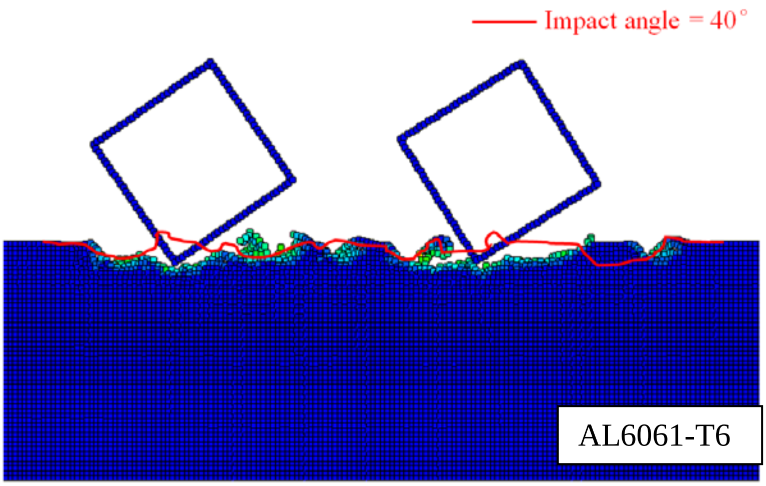

Fig. 14 Comparison of surface morphology between different impact angle

4.Discussion

The SPH has several advantages over element-based numerical methods, such as it can handle large deformation and material removal due to its Lagrangian and adaptive nature; it is relatively easy to incorporate complicated physics. For the present simulation, particle impact on ductile targets usually involves rapid deformation and quick damage, which may result in disordered particle distribution. As described in above sections, the SPH discretization procedure based on the improved algorithm is employ. Two modified algorithms may help to improve the computational accuracy. Besides, there are many other aspects affecting the accuracy, efficiency and stability of the numerical solutions, such as the choice of the smoothing function, the artificial viscosity, and the neighbouring searching strategy, etc. These aspects degrade the repeatability of numerical test to some extent and make SPH not attractive as some element-based methods. Therefore, it is essential to properly address these issues before applying the method to particular applications.

In this study, the artificial viscosity is introduced into the momentum equation to damp out the undesirable oscillations. For the value of α, Monaghan[32] selected $\alpha = 0.01$ for the free surface flow; Libersky et al.[38] selected $\alpha = 2.5$ for solid mechanics problem. Monaghan also recommended that α close to 1 may be the best choice for most cases. The other term associated with parameter β is devoted to suppress particle interpenetration at high Mach number[40], which dose not have much effect in the present simulation since the velocity (<100m/s) is small compared with the speed of sound ($\sim 10^3$). Our tests give similar results for the value of β between 0 and 2.5, which is the commonly used range recommended by researchers[38, 46]. It has been found that $\alpha = 1.0$ and $\beta = 1.0$ are proper for the present simulation in terms of suppressing numerical oscillations on one hand and leading to less unphysical energy dissipations on the other hand.

Another important aspect affecting the efficiency of the computation is the neighbouring searching procedure. Generally, the easiest way to do this job is to calculate the distance between every two possible neighbouring particles in the computation domain. However, this direct way has low efficiency because it involves a number of interactions on the order of $N \times N$. In the present work, an efficient strategy named linked-list method is adopted. It is suitable for uniformly distributed particles, which is the case for this simulation. For more details on implementing this strategy one can refer to Ref. [49].

5.Conclusion

This paper developed a 3D–SPH model to simulate surface erosion of ductile materials subjected to impacts of angular particles travelling a given velocity. In the model, both the targeted material and the rigid angular particle are discretized bymeshfree particles. Once the rigid–target interaction has been detected, contact forces are imposed to particles close to the interface. In particular, the action of the rigid particle on the target is computed through particles contact algorithm based on penalty force approach. On the contrary, the action on the rigid particle is computed by summing up all reaction forces from targeted particles which satisfy the action–reaction principle.

The SPH model, thanks to its Lagrangian and adaptive nature, has the great advantage of modeling large deformation and material removal, and does not need any specific treatment for the distorted computational domain. By incorporating the Johnson–Cook plasticity and failure model, the developed SPH model can capture the rate–dependent plastic behavior and damage behavior, which are the key components in erosion mechanisms of ductile material. Further on, chip separation caused by particle impacts is revealed and presented as a dynamic process, which is helpful in taking a close look at the fundamental mechanisms.

To solve the problem of low accuracy in standard SPH method, MLS density correction and kernel gradient correction are implemented into our SPH code. By using the density correction and artificial viscosity together, the stress oscillations in standard SPH model are effectively alleviated. And the unphysical energy dissipation of artificial viscosity is also significantly reduced by appropriately applying the MLS density correction.

The numerical analyses of angular particle impact on AL6026–T6 and OFHC Copper are applied to validate the capability and accuracy of the model.The obtained numerical results clearly demonstrate that the presented SPH model can effectively simulate particle erosion problems. The present work thus forms the basis from which the more realistic multiple particle impact erosion mechanisms can be simulated. However, the present work only simulates solid particle erosion on ductile materials. Future work will be applications in brittle materials using presented method.

References

1 P.Tangestanian, M.Papini, J.K. Spelt,Starch media blast cleaning of artificially aged paint films, Wear, 248 (1–2) (2001), 128–139.

2 Naresh Kumar, Mukul Shukla, Finite element analysis of multi–particle impact on erosion in abrasive water jet machining of titanium alloy. Journal of Computational and Applied Mathematics, 236 (18) (2012), 4600–4610.

3 S.Ariely, A.Khentov, Erosion corrosion of pump impeller of cyclic cooling water system. Engineering Failure Analysis, 13(6) (2006), 925–932.

4 Chong Y.Wong, Christopher Solnordal, Anthony Swallow, Experimental and computational modeling of solid particle erosion in a pipe annular cavity, Wear. 303 (1–2) 2013, 109–129.

5 SubhashN.Shah, Samyak Jain, Coiled tubing erosion during hydraulic fracturing slurry flow, Wear. 264 (3–4) (2008),279–290.

6 W. Zeng, J.M. Larsen, G.R. Liu,Smoothing technique based crystal plasticity finite element modeling of crystalline materials, International Journal of Plasticity. 65 (2015), 250–268.

7 M.S.EITobgy, E.Ng, M.A.Elbestawi,Finite element modeling of erosive wear. International Journal of Machine Tools and Manufacture. 45 (11) (2005), 1337–1346.

8 I.Finnie, The mechanism of erosion of ductile metals. Proceedings of the Third U.S.National Congress of Applied Mechanics. 1958, 527–532.

9 I.Finnie. Erosion of surface by solid particles. Wear.3 (2) 1960, 87–103.

10 J. Bitter, A study of erosion phenomena: part 1, Wear. 6 (1) (1963), 5–21.

11 J. Bitter, A study of erosion phenomena: part 2, Wear. 6(3) (1963), 161–190.

12 M.Takaffoli, M.Papini, Finite element analysis of single impacts of angular particles on ductile targets, Wear. 267 (1–4) (2009), 144–151.

13 M. Hashish, Modified model for erosion, Seventh International Conference on Erosion by Liquid and Solid Impact, Cambridge, England, 1987, 461–480.

14 J. Neilson, A. Gilchrist, Erosion by a stream of solid particles. Wear, 11 (2) (1968), 111–122.

15 Y.I. Oka, K.Nagahashi, Measurements of plastic strain around indentations caused by the impact of round and angular particles, and the origin of erosion, Wear.254 (12) (2003) ,1267–1275.

16 I.Hutchings, R. Winter, Particle erosion of ductile metals: a mechanism of material removal, Wear.27 (1) (1974) ,121–128.

17 H.M. Hawthorne, Y.Xie, S.K. Yick, A study of single particle–target surface interactions along a specimen in the Coriolis slurry erosion tester, Wear.253 (3–4) (2002) ,403–410.

18 G.Sundarajan, A comprehensive model for the solid particle erosion of ductile materials, Wear.149 (1–2) (1991) ,111–127

19 G.Sundararajan, P.G.Shewmon,The oblique impact of a hard ball against ductile, semi–infinite, target materials–experiment and analysis,International Journal of Impact Engineering. 6 (1) 1987, 3–22

20 Y.Tirupataiah,B.Venkataraman, G.Sundararajan,The nature of the elastic rebound of a hard ball impacting on ductile, metallic target materials, Material Science and Engineering: A. 124 (2) 1990, 133–140.
21 Rickerby DG, MacMillan NH,On the oblique impact of a rigid sphere against a rigid–plastic solid, Int. J.Mech.Sci..22 (8) (1980), 491–494.
22 G.Sundararajan, The depth of the plastic deformation beneath eroded surfaces: the influence of impact angle and velocity, particle shape and material properties. Wear. 149 (1–2) (1991), 129–153.
23 K.Shimizu, T.Noguchi, H.Seitoh, M.Okada, Y.Matsubara, FEM analysis of erosive wear, Wear. 250 (1–12) (2001), 779–784.
24 M.Junkar,B.Jurisevic, M.Fajdiga, M.Grah, Finite element analysis of single particle impact in abrasive water jet machining, International Journal of Impact Engineering. 32(7)(2006),1095–1112.
25 Griffin, A. Daadbin, S. Datta, The development of a three–dimensional finite element model for solid particle erosion on an alumina scale/MA956 substrate, Wear. 256 (9–10) (2004), 900–906.
26 P.J. Woytowitz, R.H. Richman, Modeling of damage from multiple impacts by spherical particles, Wear. 233–235 (1999), 120–133.
27 J.F. Molinari, M. Ortiz, A study of solid–particle erosion of metallic targets, International Journal of Impact Engineering. 27 (4) (2002), 347–358.
28 B. Zouari, M. Touratier, Simulation of organic coating removal by particle impact, Wear. 253 (3–4) (2002), 488–497.
29 Lucy. L. B. , A numerical approach to testing the fission hypothesis, Astronomical Journal. 82 (1977), 1013–1024.
30 Gingold. R. A, Monaghan. J. J ,Smoothed particle hydrodynamics– theory and application to non–spherical stars, Monthly Notices of the Royal Astronomical Society. 181 (1977), 375–389.
31 J. J. Monaghan, Smoothed particle hydrodynamics, Annual Review of astronomy and astrophysics. Astronomy and Astrophysics. 30 (1992), 543–574.
32 J. J. Monaghan, Simulating free surface flows with SPH, Journal of Computational Physics. 110 (2) (1994), 399–406.
33 J.R. Shao, H.Q. Li, G.R. Liu, M.B. Liu, An improved SPH method for modeling liquid sloshing dynamics,Computers & Structures, 100–101 (2012), 18–26

34 H. Takeda, S.M. Miyama, M. Sekiya, Numerical simulation of viscous flow by smoothed particle hydrodynamics, Progress of Theoretical Physics, 92 (5)(1994), 939–960.

35 J.P. Morris, P.J. Fox, Yi Zhu, Modeling low Reynolds number flows using SPH, Journal of Computational Physics.136 (1) (1997), 214–226.

36 G.R. Johnson, Robert A. Stryk, Stephen R. Beissel, SPH for high velocity impact computations, Computer Methods in Applied Mechanics and Engineering, 139 (1-4) (1996), 347–373.

37 M.B.Liu, G.R. Liu, Smoothed particle hydrodynamics(SPH): an overview and recent development, Arch Comput Methods Eng (2010)17: 25–76.

38 P.W.Randles, L.D. Libersky, Smoothed particle hydrodynamics: some recent improvement and applications,Computer Methods in Applied Mechanics and Engineering. 139 (1-4) (1996), 375–408.

39 Sonddong Shao, Edmond Y.M. Lo, Incompressible SPH method for simulating Newtonian and non–Newtonian flows with a free surface, Advances in Water Resources. 26 (7)(2003), 787–800.

40 Ha H.Bui, Ryoichi Fukagawa, KazunariSako, ShintaroOhno. Lagrangianmeshfree particles method (SPH) for large deformation and failure flows of geomaterial using elastic–plastic soil constitutive model, International Journal for Numerical and Analytical Methods in Geomechanics.32 (12) (2008), 1537–1570.

41 Yu–Fei Wang, Zhen–Guo Yang,A coupled finite element and meshfree analysis of erosive wear, Tribology International. 42 (2) (2009), 373–377.

42 M.Takaffoli, M.Papini. Material deformation and removal due to single particle impacts on ductile materials using smoothed particle hydrodynamics, Wear. (274–275) (2012), 50–59.

43 T. Belytschko, Y. Krongauz, J. Dolbow, C. Gerlach,On the completenesss of meshfree particle methods. International Journal for Numerical Methods in Engineering.43 (5) (1998), 785–819.

44 M.B. Liu, G.R. Liu, Restoring particle consistency in smoothed particle hydrodynamics, Applied Numerical Mathematics. 56 (1) (2006), 19–36.

45 R. Fatehi, M. T. Manzari, A remedy for numerical oscillations in weakly compressible smoothed particle hydrodynamics, International Journal for Numerical Methods in Fluids. 67 (9) (2011), 1100–1114.

46 G.R. Liu, M.B. Liu, Smoothed particle hydrodynamics: A meshfree particle method. World Scicentific: Singapore, 2004
47 Monaghan, J. J. ,Lattanzio. J. C., A refined particle method for astrophysical problems, Astronomy and Astrophysics, 149 (1) (1985),135–143.
48 M.B. Liu, W. P. Xie, G.R. Liu, Modeling incompressible flows using a finite particle method,Applied Mathematical Modelling . 29 (12) (2005), 1252–1270
49 G.A.Dilts, Moving–least–square–particles hydrodynamics –I. Consistency and stability, International Journal for Numerical Methods in Engineering. 44 (8) (1999), 1115–1155.
50 J. Bonet, S. Kulasegaram, Correction and stabilization of smooth particle hydrodynamics methods with applications in metal forming simulations, International Journal for Numerical Methods in Engineering. 47 (6) (2000), 1189–1214.
51 J.K. Chen, J.E. Beraun, T.C. Carney, A corrective smoothed particle method for boundary value problems in heat conduction, International Journal for Numerical Methods in Engineering. 46 (2) (1999), 231–252
52 J.K. Chen, J.E. Beraun,A generalized smoothed particle hydrodynamics method for nonlinear dynamic problems,Computer Methods in Applied Mechanics and Engineering. 190 (1–2) (2000), 225–239
53 Andrea Colagrossi, Maurizio Landrini,Numerical simulation of interfacial flows by smoothed particle hydrodynamics, Journal of Computational Physics. 191 (2) (2003), 448–475.
54 Man Hu, M.B Liu, M.W. Xie, G.R. Liu, Three–dimensional Run–out Analysis and Prediction of Flow–like Landslides using Smoothed Particle Hydrodynamics, Environmental Earth Science. August (2014).
55 Gordon. R. Johnson and William H. Cook, A constitutive model and data for metals subjected to large strains, high strain rates, and high temperatures. Proc. 7th Int. Symp.On Ballistics, Hague, Netherlands, April (1983).
56 Gordon. R. Johnson and William H. Cook,Fracture characteristics of three metals subjects to various strain, strain rate, temperatures and pressures, Engineering Fracture Mechanics, 21 (1)1985, 31–48.
57 M.Papini, J.K. Spelt,Impact of rigid angular particles with fully–plastic targets. Part I. Analysis,International Journal of Mechanical Sciences. 42 (5) (2000), 991–1006.
58 M.Papini, J.K.Spelt. Impact of rigid angular particles with fully–plastic targets, part II: Parametric study of erosion phenomena, International Journal of Mechanical Sciences. 42 (5)(2000), 1007–1025.

59 M.Papini, S.Dhar,Experimental verification of a model of erosion due to the impact of rigid single angular particles on fully plastic targets,International Journal of Mechanical Sciences. 48 (5) (2006), 469–482.

60 D.R.Lesuer, G. J. Kay, M. M. LeBlanc, Modeling large strain, high rate deformation in metals, in: Third Biennial Tri–Laboratory Engineering Conference Modeling and Simulation, Pleasanton, CA, November 3-5, 1999.

61 M. Meo, R. Vignevic, Finite element analysis of residual stress induced by shot peening process, Advances in Engineering Software, 34 (9) (2003), 569–575.

62 M.A.S Torres, H.J.CVoorwald, An evaluation of shot peening, residual stress and stress relaxation on the fatigue life of AISI 4340 steel, International Journal of Fatigue, 24 (8) (2002), 877–886.